# Numerical and Analytical solutions of Heat and Mass transfer of Casson nanofluid flow with convective boundary conditions.

Aroloye, S.J[1], Fenuga, O.J[2], Abiala, I. O[3]

[1,2,3] Department of Mathematics, Faculty of Science, University of Lagos, Nigeria

International Conference and Advanced Workshop on Modelling and Simulation of Complex System

# Introduction

- The theory of non-Newtonian fluid flow over a stretching surface has become a field of active research for the last few decades due to its wide range of applications in technology and industry. Such applications include polymer extrusion from a dye, wire drawing, the boundary layer along a liquid film in condensation processes, glass blowing, paper production, artificial fibers, hot rolling, cooling of metallic sheets or electronic chips, food stuffs, slurries and many others.

# Introduction Cont

Many researchers and scientists, Nadeem and fang (2011) analyzed the boundary layer flow over a stretching surface on various non-Newtonian models. The various non-Newtonian fluids are power-law fluids, micropolar fluids, viscoelastic fluids, Jeffrey fluid, Rivlin Ericksen fluids, Casson fluids, Walter's liquid B fluids etc. Although various types of non-Newtonian fluid models are proposed to explain the behavior, one of the most important types of non-Newtonian fluids is the Casson fluid. The Casson fluid is a plastic fluid, which yields shear stress in Constitutive equations.

# Introduction Cont

Some of the examples of Casson fluid model are jelly, soup, honey, tomato sauce, concentrated fruit juices, drilling operations, food processing, metallurgy, paints, coal in water, synthetic lubricants, manufacturing of pharmaceutical products, synovial fluids, sewage sludge and many others. Human blood is also considered as Casson fluid because of the presence of several substances like protein, fibrinogen and globin in aqueous base plasma in the blood. Human red cells from a chain like structure, known as aggregates or rouleaux. If the rouleaux behave like a plastic solid then there exists a field stress that can be identified with the constant stress in Casson fluid (2009)

# Literature Review

AZIZ [2013] carried out an analysis to discuss the steady laminar flow over a flat plate with convective boundary condition. MAKINDE and AZIZ [2015] extended the work of AZIZ [2020] by considering the MHD flow through a porous medium with buoyancy force. HAMAD et al [2019] analyzed the variable diffusivity fluid combined with heat and mass transfer in the presence of thermal boundary condition. They discussed the solution employied by LIE group method [2020].

# Literature Review Cont

Three dimensional boundary layer flow of Jeffery fluid with convective surface condition was discussed by SHEHZAD et al [2019]. HAYAT et al [2020] presented homotopic solutions of buoyancy driven flow of Maxwell fluid near a stagnation point in the presence of convective condition. Boundary layer flow of nanofluid with thermal convective boundary condition was investigated by MAKINDE and AZIZ [2018]. ALSAEDI et al [2014] extended the analysis of by considering stagnation point flow with heat generation/absorption.

# Literature Review Cont

The present investigation is focus on Heat and mass transfer of magnetohydrodynamic (MHD) Casson fliud in the presence of nanofluid, viscous dissipation, thermal radiation and magnetics effect subjected to convective boundary conditions

# Problems development

**The problem governing equations are**

$$\frac{\partial u}{\partial x}+\frac{\partial v}{\partial y}=0 \tag{1}$$

$$u\frac{\partial u}{\partial x}+v\frac{\partial u}{\partial y}=\left(1+\frac{1}{\beta}\right)\frac{\partial^2 u}{\partial y^2}-\frac{\sigma\beta_0^2}{\rho_f}u+gB_T(T-T_\infty)+gBc(C-C_\infty) \tag{2}$$

$$u\frac{\partial T}{\partial x}+v\frac{\partial T}{\partial y}=\alpha\frac{\partial^2 T}{\partial y^2}+r\left(D_B\frac{\partial C}{\partial y}\frac{\partial T}{\partial y}+\frac{D_r}{T_\infty}\left(\frac{\partial T}{\partial y}\right)^2\right)+\frac{\nu}{c_p}\left(1+\frac{1}{\beta}\right)\left(\frac{\partial u}{\partial y}\right)^2+\frac{\partial^2 q_r}{\partial y^2}+\upsilon\left(\frac{\partial u}{\partial y}\right)^2 \tag{3}$$

$$u\frac{\partial C}{\partial x}+v\frac{\partial C}{\partial y}=D_B\frac{\partial^2 C}{\partial y^2}+\frac{D_T}{T_\infty}\frac{\partial^2 T}{\partial y^2} \tag{4}$$

# Boundary conditions

The boundary conditions for the considered flow analysis are

$$u = u_w(x) = U_0 \exp\left(\frac{x}{L}\right),$$

$$v = 0, \quad -k\frac{\partial T}{\partial y} = h_1(T_f - T),$$

$$-D_B\frac{\partial C}{\partial y} = h_2(C_f - C), \quad at\ y = 0;$$

$$u \to 0, v \to 0, T \to T_\infty, C \to C_\infty, \ when\ y \to \infty \qquad (5)$$

Where $u$ and $v$ are the velocity components in the $x-$and $y-$direction; $v$ is the kinematic viscosity; $\beta$ is the Casson parameter; $\rho_f$ is the density of fluid; $\sigma$ is the Steffan-Boltzman constant; $\alpha$ is the thermal diffusivity; $r = \frac{(\rho c)_p}{(\rho c)_f}$ is the ratio of nanoparticle heat capacity and the base fluid heat capacity; $v$ is the kinematic viscosity; $c_p$ is the specific heat capacity; $D_B$ is the Brownian diffusion coefficient; $D_T$ is the thermophoretic diffusion coefficient; $k$ is the thermal conductivity; $h_1$ and $h_2$ are the heat and mass transfer coefficients, respectively; $T_\infty$ and $C_\infty$ are the ambient fluid temperature and concentration, respectively. The radiative heat flux, taking into account the Rosseland approximation, can be expressed as $q_r = \frac{4\sigma^*}{3k^*}\frac{\partial T^4}{\partial y}$

# SIMILARITY VARIABELS

$$\eta = y\sqrt{\frac{U_0}{2\nu L}}\exp\left(\frac{x}{2L}\right), \qquad u = U_0 \exp\left(\frac{x}{L}\right) f'(\eta),$$

$$v = -\sqrt{\frac{\nu U_0}{2L}}\exp\left(\frac{x}{2L}\right)(f(\eta) + \eta f'(\eta)),$$

$$A\exp\left(\frac{ax}{2L}\right)\theta(\eta) = \frac{T - T_\infty}{T_f - T_\infty}, \qquad B\exp\left(\frac{ax}{2L}\right)\phi(\eta) = \frac{C - C_\infty}{C_f - C_\infty}$$

# The equations of linear momentum, energy and concentration in dimensionless form become

$$\left(1+\frac{1}{\beta}\right)f'''+ff''-2f'^{2}-M^{2}f'+Gr\theta+Gc\phi=0 \tag{6}$$

$$\theta''+\Pr f\theta'+\Pr Nb\theta'\phi'+\Pr Nt\theta'^{2}+\Pr Ec\left(1+\frac{1}{\beta}\right)f''^{2}+Ra\,\theta=0 \tag{7}$$

$$\phi''+Lef\phi'+(N_t/N_b)\theta''=0 \tag{8}$$

*BoundaryConditions*

$$f=0,\ f'=1,\ \theta'=-Bi_1(1-\theta(0)),\ \phi'=-Bi_2(1-\phi(0)); \tag{9}$$

$$at\ \eta=0,\ f'\to 0,\theta\to 0,\phi\to 0,\ as\ \eta\to\infty$$

# Embedded Flow parameters

where $M^2 = \frac{2\sigma B_0^2 L}{(\rho_f U_0 \exp(x/L))}$ is the magnetic parameter, $\Pr = \frac{\nu}{\alpha}$ is the Prandtl number;

$Le = \frac{\nu}{D_B}$ is the Lewis number; $Nb = \frac{(\rho c)_p D_B (C_f - C_\infty)}{((\rho c)_f \nu)}$ is the Brownian motion parameter;

$Nt = \frac{(\rho c)_p D_T (T_f - T_\infty)}{((\rho c)_f \nu T_\infty)}$ is the thermophoresis parameter; $Bi_1 = (h_1 / k)\sqrt{\nu / a}$, $Bi_2 = (h_2 / D_B)\sqrt{\nu / a}$

are the Biot numbers, $Ra = \frac{16\sigma T^4}{3k^* Cp}$ is the thermal radiations, $Gc = \frac{gB_T (C_w - C_\infty)}{U_0^2}$ is the local

solutal Grashof number, $Gr = \frac{gB_T (T_f - T_\infty)}{U_0^2}$ is the local thermal Grashof number

The skin friction coefficient, the local Nusselt number and the local Sherwood number are

$C_f = \frac{r_w}{\rho_f u_w^2(x)}$, $Nu_x = \frac{x q_w}{k(T_f - T_\infty)}$, $Sh_x = \frac{x q_m}{D_B (C_f - C_\infty)}$

# Result validation

Table 1. Computation showing $f''(0)$, $\theta'(0)$, and $\phi'(0)$ for various values of embedded parameter when compared with Makinde (2010)

| | | | | | | $f''(0)$ | | $-\theta'(0)$ | | $-\phi'(0)$ | |
|---|---|---|---|---|---|---|---|---|---|---|---|
| Bi | Gr | Gc | M | Pr | Sc | Makinde (2010) | Present work | Makinde (2010) | Present work | Makinde (2010) | Present work |
| 0.1 | 0.1 | 0.1 | 0.1 | 0.72 | 0.62 | −0.402271 | −0.402262 | 0.078635 | 0.078634 | 0.3337425 | 0.3337434 |
| 1.0 | 0.1 | 0.1 | 0.1 | 0.72 | 0.62 | −0.352136 | −0.352140 | 0.273153 | 0.273152 | 0.3410294 | 0.3410293 |
| 10 | 0.1 | 0.1 | 0.1 | 0.72 | 0.62 | −0.329568 | −0.329556 | 0.365258 | 0.365258 | 0.3441377 | 0.3441376 |
| 0.1 | 0.5 | 0.1 | 0.1 | 0.72 | 0.62 | −0.322212 | −0.322220 | 0.079173 | 0.079174 | 0.3451301 | 0.3451303 |
| 0.1 | 1.0 | 0.1 | 0.1 | 0.72 | 0.62 | −0.231251 | −0.231260 | 0.079691 | 0.079692 | 0.3566654 | 0.3566653 |
| 0.1 | 0.1 | 0.5 | 0.1 | 0.72 | 0.62 | −0.026410 | −0.026421 | 0.080711 | 0.080713 | 0.3813954 | 0.3813953 |
| 0.1 | 0.1 | 1.0 | 0.1 | 0.72 | 0.62 | 0.3799184 | 0.3799183 | 0.082040 | 0.082042 | 0.4176697 | 0.4176696 |
| 0.1 | 0.1 | 0.1 | 1.0 | 0.72 | 0.62 | −0.985719 | −0.985720 | 0.074174 | 0.074172 | 0.2598499 | 0.2598498 |
| 0.1 | 0.1 | 0.1 | 5.0 | 0.72 | 0.62 | −2.217928 | −2.217930 | 0.066156 | 0.066158 | 0.1806634 | 0.1806633 |
| 0.1 | 0.1 | 0.1 | 0.1 | 1.00 | 0.62 | −0.407908 | −0.407910 | 0.081935 | 0.081938 | 0.3325180 | 0.3325181 |
| 0.1 | 0.1 | 0.1 | 0.1 | 7.10 | 0.62 | −0.421228 | −0.421225 | 0.093348 | 0.093346 | 0.3305618 | 0.3305613 |
| 0.1 | 0.1 | 0.1 | 0.1 | 0.72 | 0.78 | −0.411704 | −0.411703 | 0.078484 | 0.078483 | 0.3844559 | 0.3844558 |
| 0.1 | 0.1 | 0.1 | 0.1 | 0.72 | 2.63 | −0.453094 | −0.453092 | 0.077915 | 0.077917 | 0.7981454 | 0.7981453 |

# Casson parameter effect on the Temperature profile

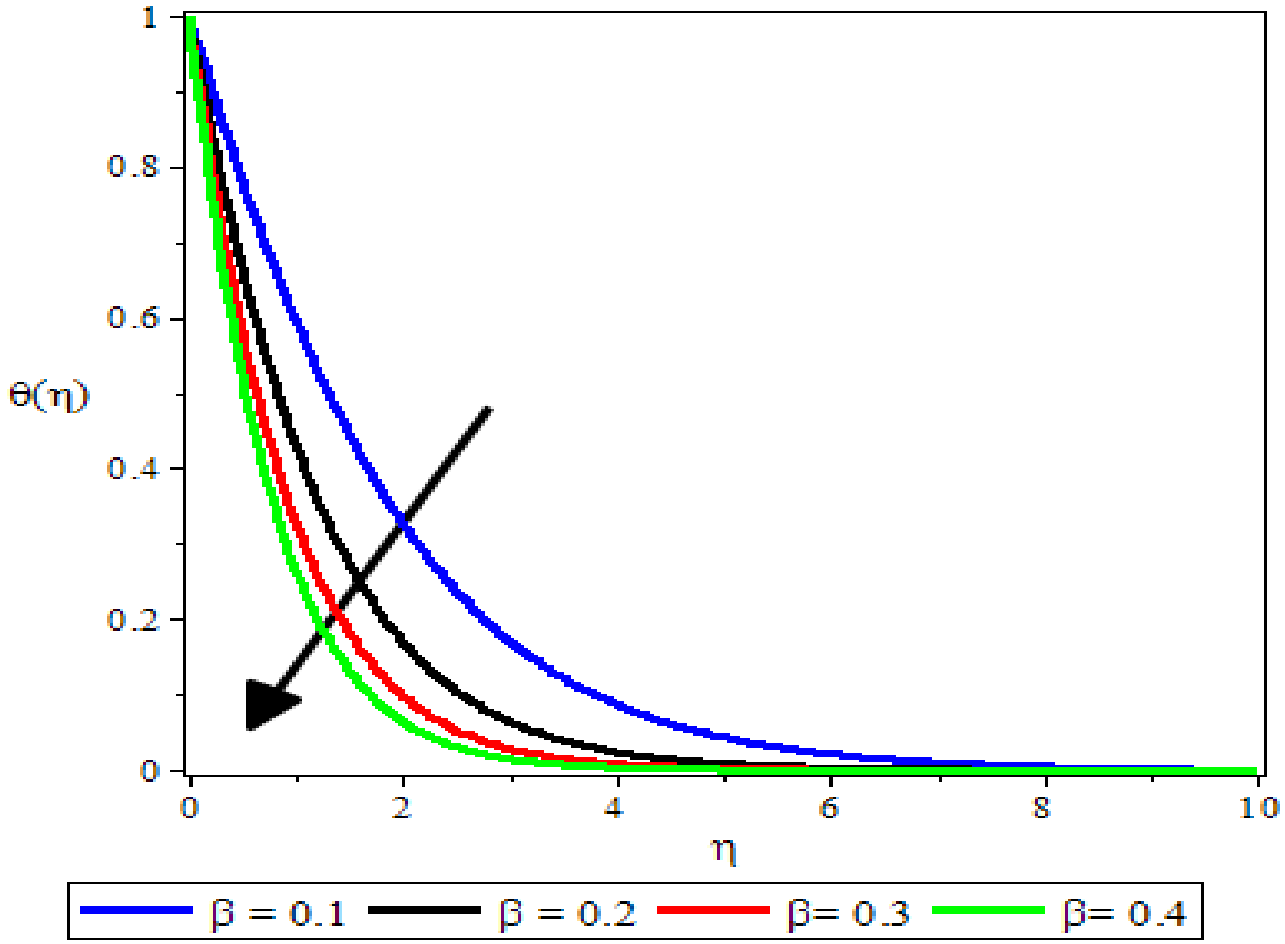

.

The figure above witnesses that the temperature and thermal boundary layer thickness decrease for the higher values of Casson parameter. Higher value of Casson parameter corresponds to a decrease in the yield stress that causes a reduction in the fluid temperature and thermal boundary layer thickness

# Magnetic effect on the velocity profiles

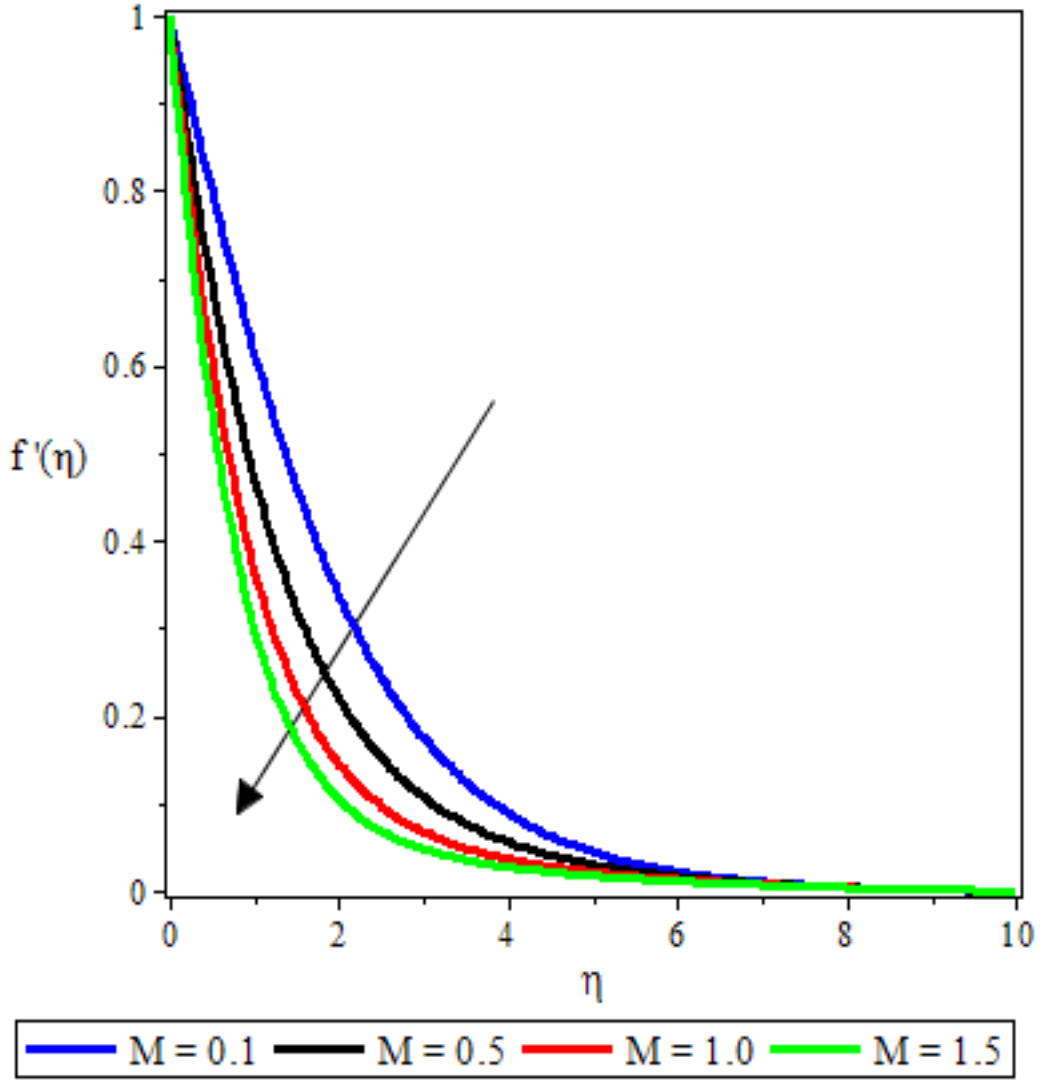

# Magnetic effect on the Temperature profiles

.

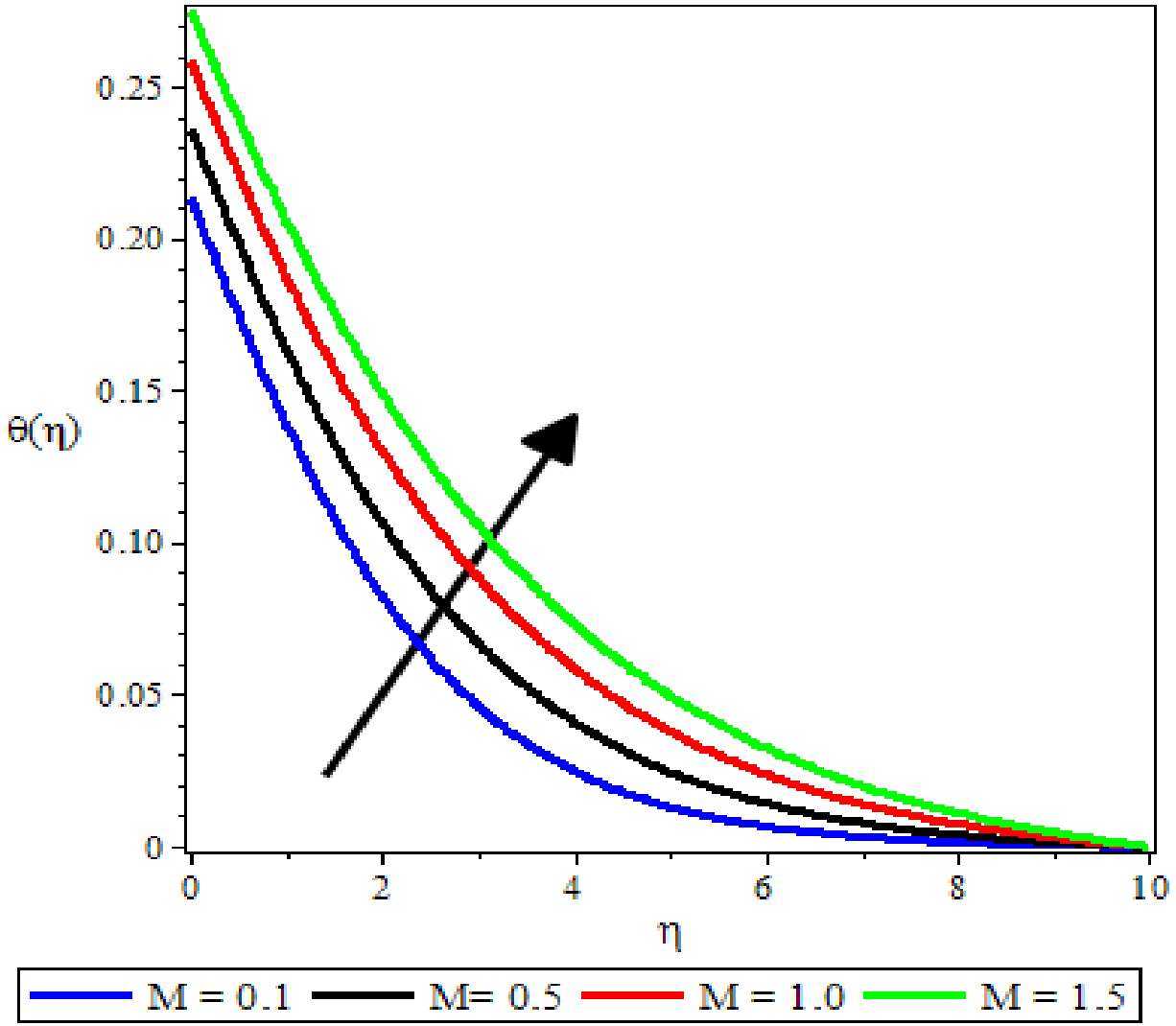

The figure above illustrates the effects of magnetic parameter on the temperature. Here, an increase in magnetic parameter leads to an enhancement in the temperature. Physically, larger value of magnetic parameter shows stronger Lorentz force. Such stronger Lorentz force is an agent providing more heat to fluid due to the fact that higher temperature and thicker thermal boundary layer thickness occur

# Magnetic effect on the Concentrations profiles

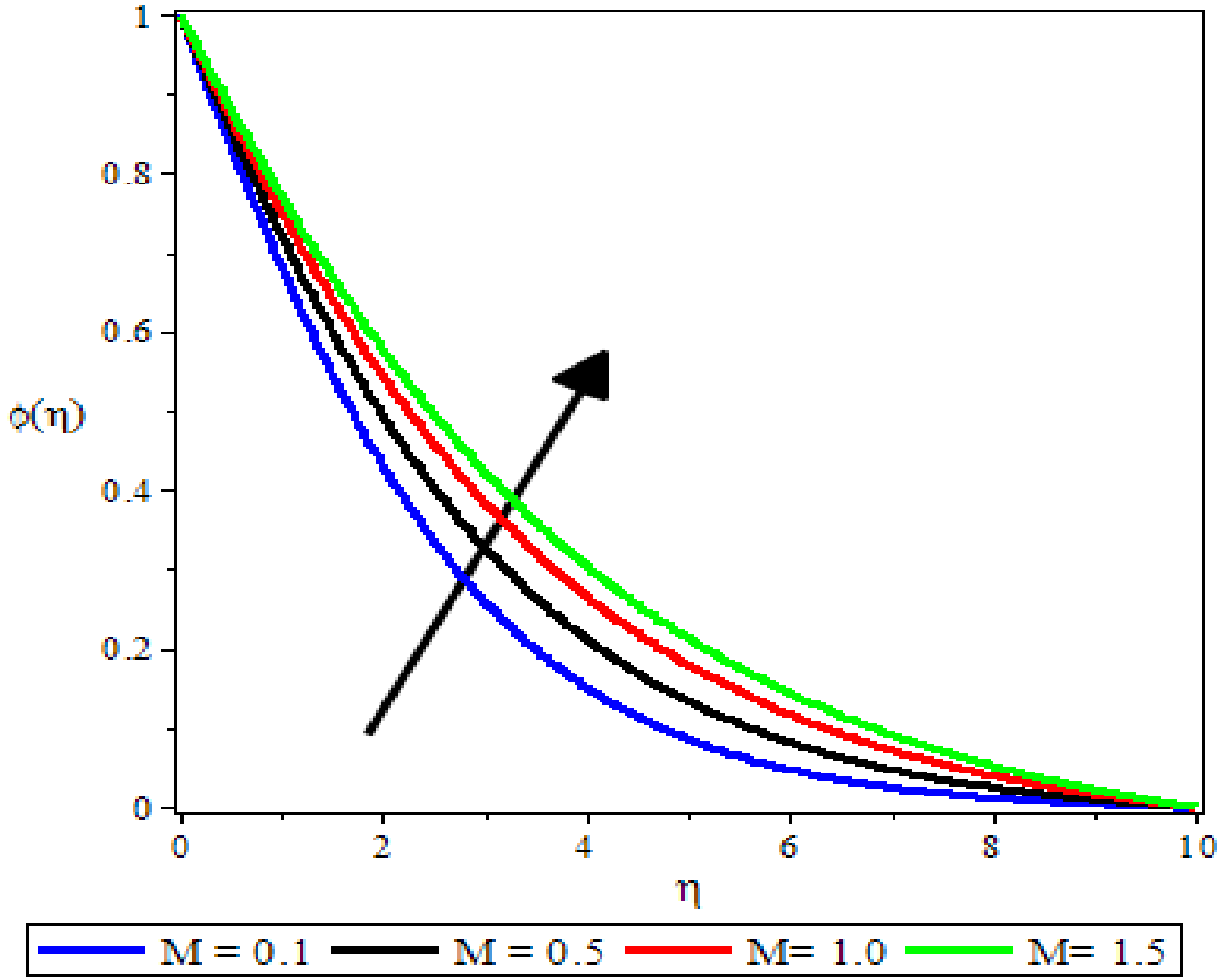

# Thermal radiation effect on the Temperature profiles

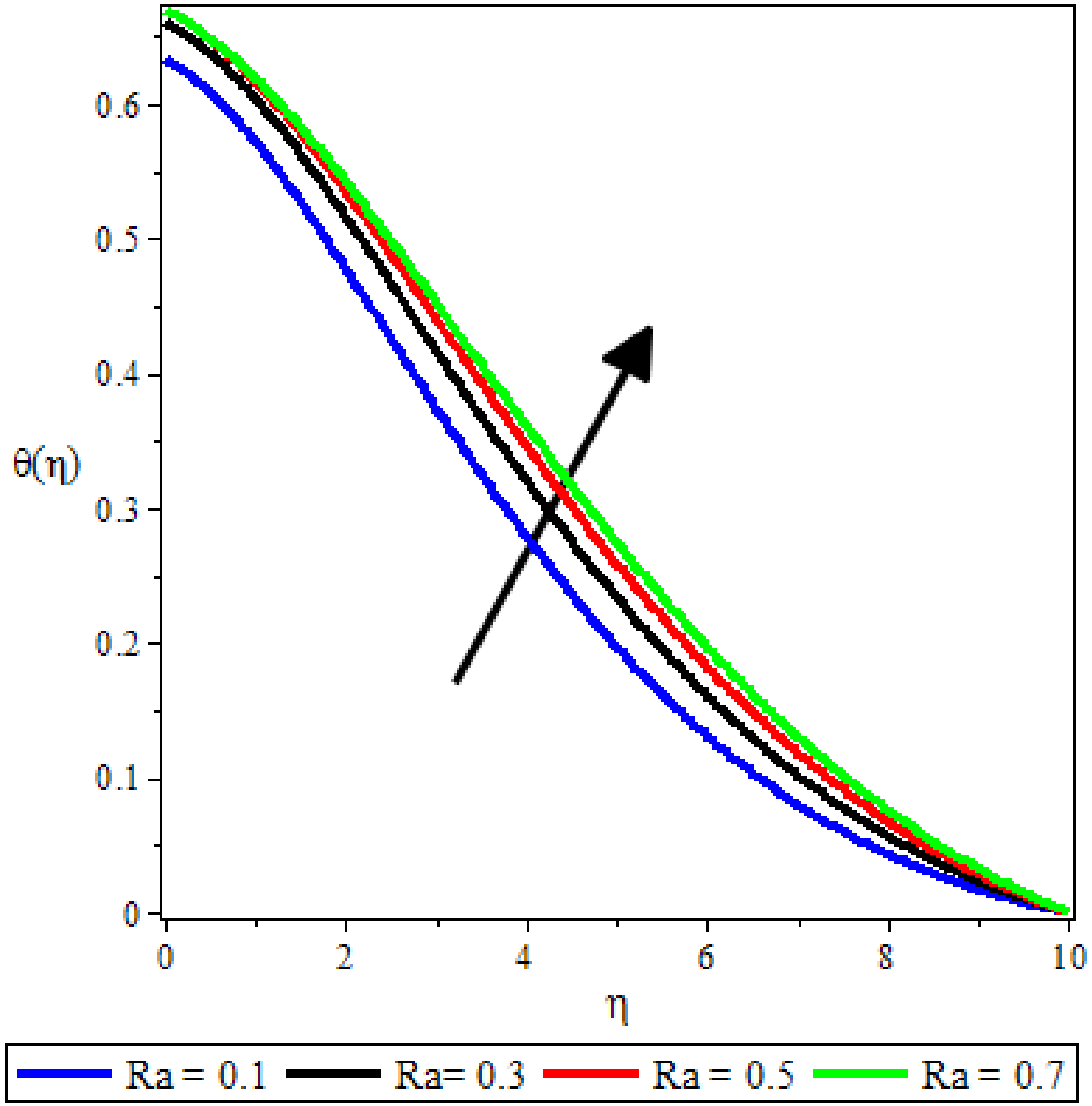

# Conclusion

- Higher value of Casson parameter leads to a decrease in the temperature and nanoparticle concentration.
- Effects of Lewis number on nanoparticle concentration are more pronounced in comparison with the temperature.
- Increasing values of Biot numbers $Bi_1$ and $Bi_2$ correspond to an increase in the fluid temperature and nanoparticle concentration.
- Temperature is enhanced for the higher values of thermophoresis and Brownian motion parameters.
- Effects of thermophoresis and Brownian motion parameters on nanoparticle concentration are quite opposite.

# References

1.KAMESWARAN P K, NARAYANA M, SIBANDA P, MURTHY P V S N. Hydromagnetic nanofluid flow due to a stretching or shrinking sheet with viscous dissipation and chemical reaction effects [J]. International Journal of Heat and Mass Transfer, 2012, 55: 7587−7595.

2. TURKYILMAZOGLU M. Exact analytical solutions for heat and mass transfer of MHD slip flow in nanofluids [J]. Chemical Engineering Science, 2012, 84: 182−187.

3. RASHIDI M M, ABELMAN S, MEHR N F. Entropy generation in steady MHD flow due to a rotating porous disk in a nanofluid [J]. International Journal of Heat and Mass Transfer, 2013, 62: 515−525.

4.HATAMI M, NOURI R, GANJI D D. Forced convection analysis for MHD Al2O3−water nanofluid flow over a horizontal plate [J]. Journal of Molecular Liquids, 2013, 187: 294−301.

5MAKINDE O D, KHAN W A, KHAN Z H. Buoyancy effects on MHD stagnation point flow and heat transfer of a nanofluid past a convectively heated stretching/shrinking sheet [J]. International Journal of Heat and Mass Transfer, 2013, 62: 526−533.